2010

Extended dislocation-based pinning mechanism in superconducting YBa2Cu3O7 films

Serhiy Pysarenko
University of Wollongong, sp973@uow.edu.au

Alexey V. Pan
University of Wollongong, pan@uow.edu.au

S X. Dou
University of Wollongong, shi@uow.edu.au

Rashmi Nigam
University of Wollongong, rnigam@uow.edu.au

Extended dislocation-based pinning mechanism in superconducting YBa2Cu3O7 films

S. V. Pysarenko, A. V. Pan, S. X. Dou, and R. Nigam

Citation: J. Appl. Phys. **107**, 09E118 (2010); doi: 10.1063/1.3365616
View online: http://dx.doi.org/10.1063/1.3365616
View Table of Contents: http://jap.aip.org/resource/1/JAPIAU/v107/i9
Published by the American Institute of Physics.

Extended dislocation-based pinning mechanism in superconducting $YBa_2Cu_3O_7$ films

S. V. Pysarenko,[a] A. V. Pan, S. X. Dou, and R. Nigam
Institute for Superconducting and Electronic Materials, University of Wollongong, Northfields Avenue, Wollongong, New South Wales 2522, Australia

(Presented 21 January 2010; received 31 October 2009; accepted 4 December 2009; published online 21 April 2010)

To describe the critical current density (J_c) as the function of applied magnetic field (B_a) in high quality $YBa_2Cu_3O_7$ (YBCO) superconducting films, the vortex pinning mechanism along the structural domain boundaries of the films is developed. The boundaries, assumed to have low misorientation angles, are quantitatively considered to consist of individual edge dislocations acting as pinning wells, rather than a continuous boundary. This extended model accurately describes the experimental $J_c(B_a)$ over the wide field and temperature ranges. Marginal deviations of the model from the experimental $J_c(B_a)$ curves are observed at high fields and temperatures where thermally activated depinning is significant. This pinning model is verified to provide precise structural properties of the films which can be obtained by other considerations. © *2010 American Institute of Physics*. [doi:10.1063/1.3365616]

Understanding of electromagnetic behavior of $YBa_2Cu_3O_7$ (YBCO) superconducting thin films at applied magnetic field (B_a) is important task of theoretical and experimental physics. Numerous attempts[1–3] to describe pinning mechanisms resulting in high J_c have led to controversial conclusions on the origin of the strong pinning in the films. The successful model[3] working over the entire B_a range has been proposed on the basis of the experimental evidence[1,4,5] indicating the significant contribution of the linear defects (dislocations) to vortex pinning. Indeed, this type of defects can pin vortices along their entire length, providing the strongest available pinning.[6–8] The other successful model[9,10] is based on the only assumption of the network of Josephson junctions governing $J_c(B_a)$ dependence in YBCO films. This assumption is unlikely to be the case in the quality YBCO films with high J_c having low angle boundaries between structural domains.[11]

In Ref. 3, it was assumed that the vortices are effectively pinned on out-of-plane extended defects [edge dislocations (EDs)], which form a network of structural domains separated by low angle boundaries (LABs). This model deals with statistical domain size distribution and the pinning width δ_c,[12,13] which characterizes the width of pinning walls formed by LABs. Basic idea is to calculate the probability to pin vortices, which form a flux-line lattice (FLL), by trapping them within the range $\delta \leq \delta_c$.

Real YBCO films demonstrate not only different domain size distribution, but also different low angles between these domains. Different angles between domains imply different spacing d between the EDs, which govern J_c in the films.[11] The spacing d has been qualitatively mentioned in the original model, however, the quantitative approach has not been developed.

In this work, we have substantially extended the statistical model by introducing more realistic the modulated pinning landscape along LABs and the rectangular (rather than square) shape of the domains. It has allowed us to explain the behavior of $J_c(B_a)$ curves with a better accuracy in the low and intermediate B_a regions. Comparison of two slightly different films verified a high sensitivity of the model to variations in microstructure.

YBCO films were grown by pulsed laser deposition (PLD) onto $SrTiO_3$ substrates[14] and by off-axis DC magnetron sputtering (MS) onto r-cut optically polished sapphire (Al_2O_3) buffered with CeO_2 layer.[15] $J_c(B_a)$ dependencies were obtained from magnetization loops measured in magnetic fields applied perpendicular to the plane of the YBCO films by employing the critical state model.

The main features of the original dislocation pinning model in YBCO films[3] are as follows. In the single vortex pinning (SVP) regime at low fields, the vortices are pinned at the individual EDs. As the applied field is increased, the vortices start interacting, forming a FLL, while $J_c(B_a)$ start decreasing. A certain vortex order in FLL means that not all the vortices can access corresponding pinning (dislocation) sites within the domain walls. The ratio between the density of pinned vortices n_p and the overall vortex density (n_v) is the key (so-called accommodation) function of the statistical approach. The J_c can be defined as follows:

$$\frac{n_p(B_a)}{n_v(B_a)} f_{\mathrm{pin}}^{\max} = f_L = J_c \phi_0, \tag{1}$$

$f_{\mathrm{pin}}^{\max}$ is the maximum pinning force,[16] f_L is the Lorentz force, and ϕ_0 is the flux quantum. Obviously, in the ideal case of the SVP regime $n_p/n_v = 1$ at $T = 0$ K.

Vortices in the FLL can be pinned along the walls of EDs within the width of $2\delta_c$.[3] Integrating the probability for a vortex in the FLL to fall within $2\delta_c$ leads to the fraction of the pinned vortices:

[a]Electronic mail: serhiy@uow.edu.au.

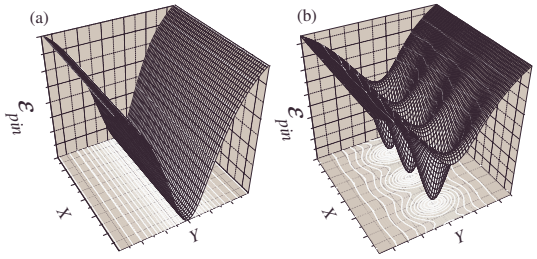

FIG. 1. (Color online) (a) The original pinning potential along the domain walls. (b) The modified potential of individual EDs [Eq. (4)].

$$\frac{n_p(B_a)}{n_v(B_a)} = \frac{J_c(B_a)}{J_c(0)} = \int_0^{2\delta_c} W dL_x dL_y + \int_{2\delta_c}^{\infty} W\left[1 - \frac{(L_x - 2\delta_c)(L_y - 2\delta_c)}{L_x L_y}\right] dL_x dL_y, \tag{2}$$

where the probability density function for a domain to have the size of $L_x \times L_y$ is given:

$$W(L_x, L_y) = L_x^{\nu-1} \frac{\exp(-L_x/\mu)}{\mu^{\nu}\Gamma(\nu)} L_y^{\nu-1} \frac{\exp(-L_y/\mu)}{\mu^{\nu}\Gamma(\nu)}. \tag{3}$$

$\Gamma(\nu)$ is the complete gamma function with μ being a scale parameter and ν — a shape parameter of the distribution.[17] Eq. (2) is different from the original model[3,18] as it deals with more flexible and realistic *rectangular* (rather than square) shape of the domains.[1]

Furthermore, we have introduced a modulated pinning potential along the pinning walls formed by LABs [Fig. 1(b)]. Indeed, the original pinning potential [Fig. 1(a)] neglects individual linear pins and any possible spacing between them. This continuous potential leads to the unjustified possibility for the vortices to slip along the boundaries if a force is applied. The role of the modulated pinning at the domain walls is particularly important in the SVP regime (otherwise, no J_c-plateau would be expected), as well as at and above the crossover from the SVP regime to the collective pinning with quite "diluted" FLL. The modulated potential is also important at higher fields simply because such pinning landscape is more realistic. However, at high fields or temperature the role of the modulated potential weakens due to thermally activated depinning and associated flux flow.

Quantitatively, the modulated pinning potential [Fig. 1(b)] created along the X-axis by an infinite chain of EDs with normal cores separated by the distance d is[16]

$$\varepsilon_{\text{pin}}(x,y) = -\varepsilon_0 \frac{2\pi^2 r_0^2}{d^2 \gamma} \frac{\sinh\,\gamma}{\cosh\,\gamma - \cos(2\sqrt{2}\pi x/d)}, \tag{4}$$

where $\gamma = [(2\sqrt{2}\pi\xi/d)^2 + (2\sqrt{2}\pi y/d)^2]^{1/2}$, $\varepsilon_0 = [\phi_0/(4\mu_0\pi\lambda)]^2$ is the flux-line energy, ξ is the temperature dependent coherence length, μ_0 is the permeability of free space, and r_0 is the radius of a normal dislocation core. The projection of this pinning potential on the X-Y plane provides the two-dimensional shape of the modulated pinning landscape, which can be adopted to the statistical model considered. Clearly, depending on d, the shape changes substantially. For $d \leq \xi$, the pining potential resembles continuous channels with negligible modulation and strong pinning across the domain walls. For $d > 2\delta_c$, the channels with reduced pinning along the domain walls essentially disappear, turning into chains of separated columnar defects. For $\delta_c \geq d > \xi$, the projected shape of the pinning potential given by Eq. (4) can be accurately approximated by the superellipse[19] $(X/\delta_c)^m + (Y/\delta_c)^n = 1$ with $m \simeq n \simeq 1.8$.

The area in the X-Y plane depends on d. This can be incorporated into the model by introducing a coefficient K_{sh}, which reflects the ratio of the pinning area between the modulated to the continuous $2\delta_c$ wide potential:

$$K_{\text{sh}}(\delta_c, d) = \frac{\delta_c \int_0^{d/2} [1 - (X/\delta_c)^m]^{1/n} dX}{\delta_c (d/2)}. \tag{5}$$

Thus, the fraction of the pinned vortices should be adjusted by taking into account K_{sh} as follows. Substituting W from Eq. (3) into Eq. (2), taking this integral, and multiplying the result by K_{sh}, we obtain

$$\frac{n_p}{n_v} = K_{\text{sh}} \left\{ 2\Gamma(\nu+2; 2\mu\delta_c) - \Gamma^2(\nu+2; 2\mu\delta_c) + \frac{4\mu\delta_c}{\nu+1}[1 - \Gamma(\nu+1; 2\mu\delta_c)][1 - \Gamma(\nu+2; 2\mu\delta_c)] - \frac{4\mu^2\delta_c^2}{(\nu+1)^2}[1 - \Gamma^2(\nu+1; 2\mu\delta_c)] \right\}, \tag{6}$$

where $\Gamma(\nu, \mu)$ is the incomplete gamma function.[17] Thus, Eq. (6) describes the normalized $J_c(B_a)$ by (i) the maximum pinning range δ_c, (ii) the domain shape factors encoded in ν and μ, and (iii) interdislocation distance d.

Note, δ_c is the maximum range for vortex pinning within the dislocation walls, which enters as a fixed parameter in the model. However, a vortex can be pinned by a dislocation as long as the vortex displacement $\delta \leq \delta_c$. The vortex displacement from the equilibrium in the FLL can be due to the applied field, temperature, and pinning landscape. It can be defined[7] through the vortex displacement energy $\varepsilon_d(\delta)$ and the FLL elastic shear modulus c_{66} as $\varepsilon_d = c_{66}\delta^2$. Thus, we can replace δ_c with δ in Eq. (6) without any assumption; moreover, we gain dependence of pinning on B_a and T encoded in $\delta(B_a, T)$.

Equation (6) provides excellent fits [Figs. 2(a) and 2(b)] to the experimental $J_c(B_a)$ curves for quality films with different microstructures *over low and intermediate field ranges*, until the flux flow becomes overwhelming, which is not accounted for by our pinning model. The independent fitting parameters are $B_0(T)$, ν, and d. B_0 is defined as the model equivalent to the characteristic field (B^*) at which $J_c(B_a)$ starts degrading with increasing B_a.[20] In YBCO films, B^* marks depinning of individual vortices resulting from the interplay between intervortex interaction, thermal activations and pinning.[20] Phenomenologically, B^* terminates the SVP regime, while within our model it can be obtained considering the following ratio:[3]

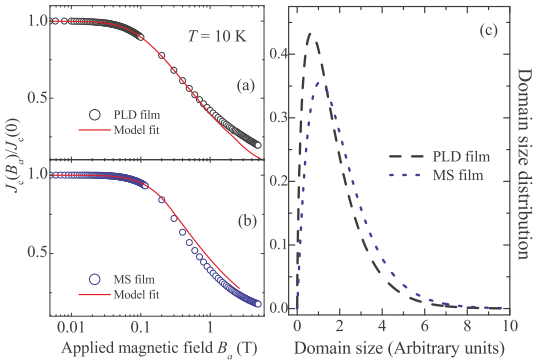

FIG. 2. (Color online) The fits of Eq. (6) to the $J_c(B_a)$ of (a) PLD and (b) MS films. (c) Domain size distribution for both films.

$$(2\delta)^2/\langle L\rangle^2 = B_0/B_a. \tag{7}$$

To understand this equality better, we consider a limiting case with the area of the *entire average* domain $\langle L\rangle^2$ has the 100% ability to pin, i.e., $(2\delta)^2/\langle L\rangle^2=1$. In this case, $J_c(B_a)$ should be independent of B_a. We can define the $\langle L\rangle^2$ from $B_0=4r_0^2\phi_0/(\mu_0\xi^2\langle L\rangle^2)$ (Refs. 3 and 16) at the condition of the maximum pinning for a vortex $\varepsilon_{\text{pin}}=\varepsilon_d$ by ignoring thermal activations.[20,21]

The results of fitting are depicted in Figs. 2(a) and 2(b) and show similar fitting parameters: PLD film $\nu=1.67$, $B_0=0.21$ T ($\langle L\rangle=276$ nm), and $d=32$ nm, and MS film $\nu=2.08$, $B_0=0.27$ T ($\langle L\rangle=244$ nm), and $d=28$ nm. We have set $\mu=1$ m^{-1}, as ν and μ are interdependent. The corresponding domain size distributions are shown in Fig. 2(c) with ν determining their broadness.

In contrast to the results obtained, PLD films are expected to result in a smaller domain size than MS films, as the growth rate for MS films is about an order magnitude slower than that for PLD films. However, to check the sensitivity and validity of our model we have chosen an optimally grown PLD film on STO substrate, and a MS film with imperfect growth conditions on CeO_2 buffered sapphire. Taking into account these growth conditions, the model exhibited an excellent sensitivity to recognize the properties of the films. In addition, the full width at half maximum of (005) peak in x-ray diffraction is larger for the MS film (0.27°) than that for the PLD film (0.19°). This indicates a better crystallinity in the PLD film with larger domains, supporting the model.

Smaller $\langle L\rangle$ and d obtained for the MS film than that for the PLD film correlate, respectively, with the lower experimental $J_c(0)$ and larger B^* than that in the PLD film.[20,21] Indeed, the higher linear defect density leads to reducing the role of intervortex interactions in SVP regime (extending B^*), whereas the larger d enables the higher current transparency with higher $J_c(0)$.[20,21] In addition, we note that $\langle L\rangle$ remarkably coincides with the individual depinning radius $r_{\text{dp}}(0)$ for both films:[20] 240 nm for PLD film and 205 nm for MS film. Note, in the model the average domain size is found, while the *experimental* $r_{\text{dp}}(0)$ returns the *onset* of effective vortex interactions and $J_c(B_a)$ degradation occurring for the smaller domains in their distribution. This result not only supports Eq. (7), but also shows that two different analysis in Ref. 20 and in this work provide essentially the same result. Finally, the difference between the model values of B_0 and the experimental $B^*\simeq 0.03$ mT for PLD film and 0.045 mT for MS film may be attributed to the different "criterion" for their definition: via Eq. (7) in the model and via 0.5% of the $J_c(B_a)$ degradation from its $J_c(0)$ value in the experiment.

In conclusion, the extended pinning model quantitatively takes into account realistic rectangular shape of the domains and modulated pinning potential of individual EDs along the LABs in YBCO films. The model accurately describes the entire experimental $J_c(B_a)$ behavior and provides the structural parameters of the films with the high accuracy and sensitivity. The sensitivity has been verified on two different YBCO films.

This work is financially supported by the Australian Research Council.

[1] F. C. Klaassen, G. Doornbos, J. M. Huijbregtse, R. C. F. van der Geest, B. Dam, and R. Griessen, Phys. Rev. B **64**, 184523 (2001).
[2] C. J. van der Beek, M. Konczykowski, A. Abal'oshev, I. Abal'osheva, P. Gierlowski, S. J. Lewandowski, M. V. Indenbom, and S. Barbanera, Phys. Rev. B **66**, 024523 (2002).
[3] V. Pan, Y. Cherpak, V. Komashko, S. Pozigun, C. Tretiatchenko, A. Semenov, E. Pashitskii, and A. V. Pan, Phys. Rev. B **73**, 054508 (2006).
[4] V. M. Pan, A. L. Kasatkin, V. L. Svetchnikov, and H. W. Zandbergen, Cryogenics **33**, 21 (1993).
[5] Yu. V. Fedotov, S. M. Ryabchenko, É. A. Pashitskiĭ, A. V. Semenov, V. I. Vakaryuk, V. M. Pan, and V. S. Flis, Low Temp. Phys. **28**, 172 (2002).
[6] L. Krusin-Elbaum, L. Civale, G. Blatter, A. D. Marwick, F. Holtzberg, and C. Feild, Phys. Rev. Lett. **72**, 1914 (1994).
[7] G. Blatter, M. V. Feigel'man, V. B. Geshkenbein, A. I. Larkin, and V. M. Vinokur, Rev. Mod. Phys. **66**, 1125 (1994).
[8] J. M. Huijbregtse, B. Dam, R. C. F. van der Geest, F. C. Klaassen, R. Elberse, J. H. Rector, and R. Griessen, Phys. Rev. B **62**, 1338 (2000).
[9] E. Mezzetti, R. Gerbaldo, G. Ghigo, L. Gozzelino, B. Minetti, C. Carmelingo, A. Monaco, G. Cuttone, and A. Rovelli, Phys. Rev. B **60**, 7623 (1999).
[10] G. Ghigo, A. Chiodoni, R. Gerbaldo, L. Gozzelino, E. Mezzetti, B. Minetti, C. Camerlingo, G. Cuttone, and A. Rovelli, Supercond. Sci. Technol. **12**, 1059 (1999).
[11] H. Hilgenkamp and J. Mannhart, Rev. Mod. Phys. **74**, 485 (2002).
[12] A. Gurevich and E. A. Pashitskii, Phys. Rev. B **57**, 13878 (1998).
[13] V. M. Pan and A. V. Pan, Low Temp. Phys. **27**, 732 (2001).
[14] A. V. Pan, S. Pysarenko, and S. X. Dou, Appl. Phys. Lett. **88**, 232506 (2006).
[15] D. A. Luzhbin, A. V. Pan, V. A. Komashko, V. S. Flis, V. M. Pan, S. X. Dou, and P. Esquinazi, Phys. Rev. B **69**, 024506 (2004).
[16] E. A. Pashitskiĭ and V. I. Vakaryuk, Low Temp. Phys. **28**, 11 (2002).
[17] R. V. Hogg and A. T. Craig, *Introduction to Mathematical Statistics*, 4th ed. (Macmillan, New York, 1978).
[18] V. M. Pan, E. Pashitskii, S. M. Ryabchenko, V. A. Komashko, A. V. Pan, S. X. Dou, A. V. Semenov, C. G. Tretiatchenko, and Yu. V. Fedotov, IEEE Trans. Appl. Supercond. **13**, 3714 (2003).
[19] J. Whitfield, *Nature Science Update* (Scientific American, New York, 2003).
[20] A. V. Pan and S. X. Dou, Phys. Rev. B **73**, 052506 (2006).
[21] A. V. Pan, Y. Zhao, M. Ionescu, S. X. Dou, V. A. Komashko, V. S. Flis, and V. M. Pan, Physica C **407**, 10 (2004).